

Subthreshold and near-threshold kaon and antikaon production in proton-nucleus reactions

A. V. Akindinov^a, M. M. Chumakov^a, M. M. Firoozabadi^b,
Yu. T. Kiselev^a, A. N. Martemyanov^a, E. Ya. Paryev^c,
V. A. Sheinkman^a, Yu. V. Terekhov^a, and V. I. Ushakov^a

^a*Institute for Theoretical and Experimental Physics,
Moscow 117218, Russia*

^b*Department of Physics, Birjand University,
Birjand 9717914141, Iran*

^c*Institute for Nuclear Research, Russian Academy of Sciences,
Moscow 117312, Russia*

May 24, 2018

Abstract

The differential production cross sections of K^+ and K^- mesons have been measured at the ITEP proton synchrotron in $p+Be$, $p+Cu$ collisions under lab angle of 10.5° , respectively, at 1.7 and 2.25, 2.4 GeV beam energies. A detailed comparison of these data with the results of calculations within an appropriate folding model for incoherent primary proton–nucleon, secondary pion–nucleon kaon and antikaon production processes and processes associated with the creation of antikaons via the decay of intermediate phi mesons is given. We show that the strangeness exchange process $YN \rightarrow NNK^-$ gives a small contribution to the antikaon yield in the kinematics of the performed experiment. We argue that in the case when antikaon production processes are dominated by the channels with KK^- in the final state, the cross sections of the corresponding reactions are weakly influenced by the in-medium kaon and antikaon mean fields.

1. Introduction

The study of the kaon and antikaon production in proton-nucleus collisions at incident energies near or below the free nucleon-nucleon thresholds has received considerable interest in recent years (see, for example, [1–27]). This interest has been particularly motivated by the hope to extract from this study information about both the intrinsic properties of target nuclei (such as high-momentum components of the nuclear wave function) and the in-medium kaon and antikaon properties at the density of ordinary nuclei (mean-field nuclear potentials, their momentum dependencies). Evidently, to draw the firm conclusions on these properties from proton-induced reactions it is of principal importance to disentangle reliably the underlying reaction mechanisms, since if the ones are clearly identified the above quantities can be fixed by comparison with the data. Therefore, we will focus in this study on the different elementary processes that lead to the kaon and antikaon production at beam energies close to their production thresholds in free NN collisions (1.58 GeV for K^+ creation and 2.5 GeV for K^- creation in these collisions).

Until now, a lot of data on total [1] and double differential [2–8, 18] K^+ production cross sections in proton-nucleus collisions at bombarding energies between 0.8 and 2.9 GeV has been collected. Whereas the experimental K^+ spectra have been taken [2, 3, 4, 18] mostly at laboratory emission angles $\geq 15^\circ$, only in two experiments [5, 6–8] the kaon yields have been obtained at forward angles ($< 15^\circ$). In the experiment [6–8], K^+ mesons were measured at laboratory angles $< 12^\circ$ and for momenta in the restricted range of 150–600 MeV/c, while in the experiment [5], kaons with an emission angle of 10.5° and a fixed momentum of 1.28 GeV/c were detected. In this respect, it is highly desirable and useful to measure differential K^+ production cross sections in pA interactions at beam energies below or close to the nucleon-nucleon threshold at forward emission angles and for the momenta ranging from ~ 0.6 to ~ 1.0 – 1.3 GeV/c, since such data in combination with the available differential data may help to shed light on the mechanism of subthreshold and near-threshold kaon creation in these interactions.

As far as the production of K^- mesons on nuclei by protons at incident energies near or below NN-threshold is concerned, only a few data exist nowadays [14–18]. K^- production has been investigated at KEK for C and Cu targets at initial energies between 3.5 and 5.0 GeV by inclusively measuring K^- at 5.1° for momentum of 1.5 GeV/c [14]. Energy dependence of the inclusive invariant cross section for the production of antikaons with momentum of 0.8 GeV/c at an angle of 24° by protons on carbon nuclei has been measured at JINR in the region of beam energies of 3.6–8 GeV [15]. An analogous dependence, but for K^- mesons with momentum of 1.28 GeV/c and an emission angle of 10.5° , was obtained at ITEP using proton energies from 2.25 to 2.92 GeV and targets Be, Al, Cu [16, 17]. The K^- momentum spectra from reactions $p + A \rightarrow K^- + X$ with $A=C$ and Au at laboratory angles from 40° to 56° and bombarding energies of 2.5 and 3.5 GeV have been measured at GSI by the KaoS Collaboration [18]. So, up to now, there exist no data on the antikaon momentum spectra from proton-nucleus collisions at beam energies below the absolute threshold for free NN interactions. It should be pointed out that the near-threshold K^- production in pA reactions is studied presently at the accelerator COSY [28].

This paper presents the K^+ and K^- momentum distributions at an angle of 10.5° in the lab frame on Be, Cu target nuclei measured at ITEP at initial proton kinetic energies of 1.7 and 2.25, 2.4 GeV, respectively, as well as their analysis within an appropriate folding model for incoherent primary and secondary elementary (anti)kaon production processes. The inclusive K^+ meson production will be analyzed by us with respect to the commonly used [3, 5, 9, 10, 12, 13, 24–27] one-step ($pN \rightarrow K^+YN$, $Y = \Lambda, \Sigma$) and two-step ($pN \rightarrow \pi X$, $\pi N \rightarrow K^+Y$) incoherent production processes. The inclusive rarer K^- meson creation will be described not only by the considering the conventional direct ($pN \rightarrow NNKK^-$) and two-step ($pN \rightarrow \pi X$, $\pi N \rightarrow NKK^-$) antikaon production processes [17, 19–23], but also with accounting for the new elementary reaction channels: $pN \rightarrow pN\phi$, $pn \rightarrow d\phi$, $\phi \rightarrow K^+K^-$; non- ϕ $pn \rightarrow dK^+K^-$. It should be noted that the total cross sections of

the elementary reactions $pp \rightarrow pp\phi$, $pn \rightarrow d\phi$, non- ϕ $pn \rightarrow dK^+K^-$, needed for our analysis, have been recently measured in the threshold region by the ANKE-at-COSY Collaboration [29, 30, 31]. In addition to the considered by us processes, K^- mesons can be produced also in the two-step reactions $pN \rightarrow K^+YN$ followed by $YN \rightarrow NNK^-$ or $Y\pi \rightarrow NK^-$. In Ref. [18,21] was found that in proton-nucleus collisions at 2.5 GeV beam energy the contribution of the above strangeness exchange processes to the cross section for antikaon production on heavy targets at large angles is essential. We show that the strength of this channel depends on the kinematical conditions of the particular experiment and the strangeness exchange processes appears to be unimportant in the kinematics of the present experiment.

The processes of the kaon and antikaon production from nuclei can also be influenced by their nuclear self-energies [10, 20, 32]. Since the K^+ attractive nuclear potential manifests itself only in the low momentum range less than 0.3-0.4 GeV/c [7,8,9] we shall neglect it in the calculation of the production of kaons with momenta of more than 0.6 GeV/c in the $pN \rightarrow K^+YN$ ($Y = \Lambda, \Sigma$) reactions in the near threshold and above threshold proton energy range of 1.5 - 2.0 GeV. The role of the K^+ potential becomes important at deep subthreshold energies [10]. We argue below that the cross sections of the reactions with KK^- in the final state like $pN \rightarrow NNKK^-$, $pn \rightarrow dKK^-$, $\pi N \rightarrow NKK^-$; $pN \rightarrow pN\phi$, $pn \rightarrow d\phi$, $\phi \rightarrow K^+K^-$ have only low sensitivity to the in-medium kaon and antikaon mean fields because they act in the opposite directions.

2. Experiment

The experiment was carried out with internal proton beam of the 10 GeV ITEP synchrotron irradiating Be and Cu strip targets of 50–100 micron thick. Initial proton energy was known within the accuracy of 5 MeV and was controlled by permanent measurement of the accelerating frequency. Secondary particles produced in the momentum range from 0.6 to 1.3 GeV/c were detected at fixed emission angle of 10.5° in lab frame by Focusing Hadron Spectrometer (FHS) consisting of two bending dipole and two pairs of quadrupole magnets. Momentum and angular acceptance of the magnetic channel are $\Delta p/p = \pm 1\%$ and 0.8 msr, correspondingly. Two multiwire proportional chambers located at the second focus of magnetic system served for monitoring of the beam position during the data taking. The particle identification system included the differential Cherenkov counter [33] and two-stage TOF system based on the scintillation counters.

The kaon and antikaon selection in the momentum range from 0.6 to 1 GeV/c was performed by using the quartz radiator of 4×6 cm² size and 1.6 cm thick with the refraction index $n = 1.47$ at $\lambda = 400$ nm. The photons emitted by the kaons in radiator were detected by the remotely controlled ring consisting of 12 photomultipliers FEU-130. For each detected momentum the differential Cherenkov counter was adjusted, using the mechanisms for lengthwise and angular PM movement, in order to achieve the highest possible efficiencies. The kaon selection criterion incorporated the requirement that 6 PMs of the ring were fired. The data on a larger number of fired photomultipliers (8, 10 and 12) were also available. The identification reliability increased with an increasing number of operated PMs, although, in this case, the detection efficiency decreased. Depending on the background level, various data sets with different number of fired photomultipliers were used in further analysis. Kaon detection efficiency varied from 65% to 95% depending on the number of operated PMs; this efficiency was periodically tested in special measurements using the protons with the same velocity. The Cherenkov counter velocity resolution was equal to 0.02. The totally reflected photons produced by pions reached the top and bottom surfaces of the radiator and then were detected by two optically coupled photomultipliers FEU-115. The signals from these photomultipliers were used to suppress the pion background with the anticoincidence channel. The pion rejection ability of 100 was reached in the 0.5–1.0 GeV/c kaon momentum range. At higher momenta the K^+ and K^- selection was performed with Cherenkov counter used in our previous

measurements [5,17]. The time-of-flight measurements were performed at two bases of 11 and 17 meters length. Two photomultipliers XP2020 mounted on both sides of each scintillator were used for the TOF measurements and provided the mean-timer signals. The time resolution of the system did not exceed 300 ps (FWHM). Our trigger for the hardware antikaon selection includes the signals from six photomultipliers of Cherenkov counters, the signals from TOF system and absence of the anticoincidence signals. The antikaon identification was quite reliable up to the value of K^-/π^- ratio equal to $1/2 \cdot 10^6$ at the downstream of the TOF counter. The K^+ and K^- misidentification was less than 5% for the most of data and did not exceed 10% at the lowest incident proton energy of 2.25 GeV.

Secondary (anti)kaons and pions were detected simultaneously. The measured meson yields were corrected for the losses due to their nuclear interactions and multiple scattering in the material of the spectrometer, detector efficiencies and meson in-flight decay at the distance of 30 meters from the production target to the second focus of the magnetic channel. The measurements of the K/π ratios covered the momentum range from 0.6 to 1.3 GeV/c. Absolute values of the K^+ and K^- production cross sections on different nuclear targets were normalized to the corresponding π^+ and π^- cross sections which were determined in special measurements in which the pion flux was measured simultaneously with the flux of the protons traversing the sandwich type targets made of thin Al foil and Be or Cu foils. The determination of the proton flux was performed by measurement of induced γ -activity in the reaction $p + {}^{27}\text{Al} \rightarrow {}^{24}\text{Na}^* + X$. The cross section of this reaction is known with accuracy of 6%. The resulting uncertainty of the absolute normalization of the invariant (anti)kaons cross sections was estimated as 20%.

The K^+ production data were taken at initial proton kinetic energy of 1.7 GeV, while the K^- creation data were obtained at two beam energies of 2.25 and 2.4 GeV. All cross sections presented in Tables 1 and 2 do not include the errors of the absolute normalization of the data.

Table 1. Invariant cross sections [$\text{GeV}\mu\text{b}/(\text{GeV}/c)^3$] for K^+ production at kinetic proton energy of 1.7 GeV and at a lab angle of 10.5°

p, GeV/c	0.675	0.806	0.940	1.05	1.15	1.28	
$Ed^3\sigma/d^3p$	121±18	104±16	43.6±6.5	10.7±1.6	2.80±0.42	0.072±0.018	Be
$Ed^3\sigma/d^3p$	308±46	212±32	87.7±13.2	33.3±5.0	8.41±1.26	0.34±0.09	Cu

Table 2. Invariant cross sections [$\text{GeVnb}/(\text{GeV}/c)^3$] for K^- production at kinetic proton energy $\epsilon_0=2.25, 2.4$ GeV and at a lab angle of 10.5°

p, GeV/c	0.640	0.807	0.940	1.05	1.14	1.28	
$Ed^3\sigma/d^3p$ $\epsilon_0 = 2.25$ GeV	3200±560	1600±240	480±80	120±18	40±6	4.7±1.2	Be
$Ed^3\sigma/d^3p$ $\epsilon_0 = 2.4$ GeV	8530±1500	4555±700	2216±380	660±100	252±40	42±6	Be
$Ed^3\sigma/d^3p$ $\epsilon_0 = 2.4$ GeV	39400±8500	18300±2800	6475±900	2800±440	921±150	197±31	Cu

In Fig. 1 the measured K^+ and K^- cross sections on the beryllium target are presented as a function of the radial Feynman variable X_F^R . The variable $X_F^R = P^*/P_{max}^* = \sqrt{(P_l^{*2} + P_t^{*2})}/P_{max}^*$, where P_l^* and P_t^* are longitudinal and transverse components of the meson momentum in the proton-nucleus center-of-mass system and P_{max}^* stands for its maximum momentum. It is seen that the cross sections for the kaon and antikaon production at near threshold and especially subthreshold collision energies drastically decrease with X_F^R . High momentum parts of the meson spectra for $X_F^R > 0.5$ follow the dependence $E d^3\sigma/d^3p \sim (1 - X_F^R)^\delta$ with the value of exponent $\delta > 4$.

3. Analysis of the data. The model and inputs

3.1. Direct K^+ and K^- production mechanisms

The direct non-resonant production of K^+ and K^- mesons in pA collisions at incident energies of our interest (up to 2.4 GeV) can occur due to the Fermi motion of nuclear nucleons in the following elementary processes with the lowest thresholds:

$$p + N \rightarrow K^+ + \Lambda + N, \quad (1)$$

$$p + N \rightarrow K^+ + \Sigma + N; \quad (2)$$

$$p + N \rightarrow N + N + K + K^-, \quad (3)$$

$$p + n \rightarrow d + K^+ + K^-, \quad (4)$$

where K stands for K^+ or K^0 for the specific isospin channel. The invariant inclusive cross sections for the production on nucleus with atomic mass number A K^+ and K^- mesons with the total energies E_{K^+} and E_{K^-} and momenta \mathbf{p}_{K^+} and \mathbf{p}_{K^-} at small laboratory emission angles from the primary proton-induced reaction channels (1)–(4) can be presented as follows [17]¹:

$$E_{K^+} \frac{d\sigma_{pA \rightarrow K^+ X}^{(\text{prim})}(\mathbf{p}_0)}{d\mathbf{p}_{K^+}} = I_{K^+}[A] \times \quad (5)$$

$$\left\{ \left\langle E_{K^+} \frac{d\sigma_{pN \rightarrow K^+ \Lambda N}(\mathbf{p}_0, \mathbf{p}_{K^+})}{d\mathbf{p}_{K^+}} \right\rangle + \left\langle E_{K^+} \frac{d\sigma_{pN \rightarrow K^+ \Sigma N}(\mathbf{p}_0, \mathbf{p}_{K^+})}{d\mathbf{p}_{K^+}} \right\rangle \right\},$$

$$E_{K^-} \frac{d\sigma_{pA \rightarrow K^- X}^{(\text{prim})}(\mathbf{p}_0)}{d\mathbf{p}_{K^-}} = I_{K^-}[A] \times \quad (6)$$

$$\left\{ \left\langle E_{K^-} \frac{d\sigma_{pN \rightarrow NNKK^-}(\mathbf{p}_0, \mathbf{p}_{K^-})}{d\mathbf{p}_{K^-}} \right\rangle + \frac{N}{A} \left\langle E_{K^-} \frac{d\sigma_{pn \rightarrow dK^+K^-}(\mathbf{p}_0, \mathbf{p}_{K^-})}{d\mathbf{p}_{K^-}} \right\rangle \right\},$$

where

$$I_h[A] = 2\pi A \int_0^\infty r_\perp dr_\perp \int_{-\infty}^{+\infty} dz \rho(\sqrt{r_\perp^2 + z^2}) \times \quad (7)$$

$$\times \exp \left[-\sigma_{pN}^{\text{in}} A \int_{-\infty}^z \rho(\sqrt{r_\perp^2 + x^2}) dx - \sigma_{hN}^{\text{tot}}(p_h) A \int_z^{+\infty} \rho(\sqrt{r_\perp^2 + x^2}) dx \right],$$

$$\sigma_{hN}^{\text{tot}}(p_h) = (Z/A)\sigma_{hp}^{\text{tot}}(p_h) + (N/A)\sigma_{hn}^{\text{tot}}(p_h) \quad (8)$$

¹We can neglect in the energy domain of our interest the additional contribution of the K^+ production processes (3), (4) to the kaon creation cross section (5) due to their larger production thresholds in pN collisions.

and

$$\left\langle E_{K^+} \frac{d\sigma_{pN \rightarrow K^+YN}(\mathbf{p}_0, \mathbf{p}_{K^+})}{d\mathbf{p}_{K^+}} \right\rangle = \int n(\mathbf{p}_t) d\mathbf{p}_t \times \quad (9)$$

$$\left[E_{K^+} \frac{d\sigma_{pN \rightarrow K^+YN}(\sqrt{s}, \mathbf{p}_{K^+})}{d\mathbf{p}_{K^+}} \right],$$

$$\left\langle E_{K^-} \frac{d\sigma_{pN \rightarrow NNKK^-(pn \rightarrow dK^+K^-)}(\mathbf{p}_0, \mathbf{p}_{K^-})}{d\mathbf{p}_{K^-}} \right\rangle = \int n(\mathbf{p}_t) d\mathbf{p}_t \times \quad (10)$$

$$\left[E_{K^-} \frac{d\sigma_{pN \rightarrow NNKK^-(pn \rightarrow dK^+K^-)}(\sqrt{s}, \mathbf{p}_{K^-})}{d\mathbf{p}_{K^-}} \right].$$

Here, $E_{K^+} d\sigma_{pN \rightarrow K^+YN}(\sqrt{s}, \mathbf{p}_{K^+})/d\mathbf{p}_{K^+}$ and $E_{K^-} d\sigma_{pN \rightarrow NNKK^-(\sqrt{s}, \mathbf{p}_{K^-})}/d\mathbf{p}_{K^-}$, $E_{K^-} d\sigma_{pn \rightarrow dK^+K^-}(\sqrt{s}, \mathbf{p}_{K^-})/d\mathbf{p}_{K^-}$ are the off-shell invariant inclusive cross sections for K^+ and K^- production in reactions (1), (2) and (3), (4), respectively; $\rho(\mathbf{r})$ and $n(\mathbf{p}_t)$ are the density and internal nucleon momentum distribution normalized to unity; \mathbf{p}_t is the momentum of the struck target nucleon just before the collision; σ_{pN}^{in} and $\sigma_{hp(hn)}^{\text{tot}}$ are the inelastic and total cross sections of free pN and hp (hn) interactions; Z and N are the numbers of protons and neutrons in the target nucleus; \mathbf{p}_0 is the momentum of the initial proton; s is the pN center-of-mass energy squared. The expression for s is:

$$s = (E_0 + E_t)^2 - (\mathbf{p}_0 + \mathbf{p}_t)^2, \quad (11)$$

where E_0 and E_t are the total energies of the projectile proton and the struck nucleon, respectively. The total energy E_t of the off-shell intranuclear nucleon is related to its momentum \mathbf{p}_t within the considered model as follows [5, 17]:

$$E_t = m_N - \frac{\mathbf{p}_t^2}{2M_{A-1}} - \epsilon. \quad (12)$$

Here, m_N is the nucleon mass, M_{A-1} is the mass of the recoiling target nucleus in its ground state, and the separation energy ϵ is taken as equal to 2 MeV.

In eqs. (5) and (6) it is assumed that the corresponding K^+ and K^- meson production cross sections in pp and pn interactions are the same [3, 12, 17, 19, 22]. The quantities $I_{K^+}[A]$ and $I_{K^-}[A]$ in these equations describe the attenuation of the proton beam as well as the distortion of the outgoing kaons and antikaons in their ways out of the nucleus. When calculating them according to the eq. (7), we use $\sigma_{pN}^{\text{in}} = 30$ mb for the considered projectile proton energies [12, 22], we adopt also $\sigma_{K^+p}^{\text{tot}} = \sigma_{K^+n}^{\text{tot}} = 12$ mb for all kaon momenta of our interest [34], and for the antikaon–nucleon total cross sections $\sigma_{K^-p}^{\text{tot}}(p_{K^-})$, $\sigma_{K^-n}^{\text{tot}}(p_{K^-})$ as functions of the K^- momentum p_{K^-} we employ the respective parametrizations suggested in [35]². The nuclear density $\rho(\mathbf{r})$ for the Be and C target nuclei of interest is given by the harmonic oscillator distribution, whereas the density for the Cu nucleus is specified by the Woods-Saxon distribution [22, 37].

In the expressions (9) and (10), entering into the eqs. (5) and (6), the differential cross sections for the production of K^+ and K^- mesons in a collision of a proton with an intranuclear nucleon, having momentum \mathbf{p}_t , are folded with the internal nucleon momentum distribution $n(\mathbf{p}_t)$. This distribution was previously determined by fitting the K^+ production cross sections in pA reactions at near-threshold and subthreshold initial energies [5]. It was assumed to be in the form

$$n(\mathbf{p}_t) = \frac{1}{(2\pi)^{3/2}(1+h)} \left[\frac{1}{\sigma_1^3} \exp(-p_t^2/2\sigma_1^2) + \frac{h}{\sigma_2^3} \exp(-p_t^2/2\sigma_2^2) \right]. \quad (13)$$

Here, $h = 0.12$, $\sigma_2 = 220$ MeV/c for the Be, C and Cu target nuclei of present interest; $\sigma_1 = 132$ and 146 MeV/c for the Be, C and Cu nuclei, respectively.

²At antikaon momenta $p_{K^-} \leq 0.63$ GeV/c we use the following relation $\sigma_{K^-n}^{\text{tot}}(p_{K^-}) = 0.8\sigma_{K^-p}^{\text{tot}}(p_{K^-})$ [36].

Let us now specify the off-shell invariant inclusive cross sections $E_{K^+} d\sigma_{pN \rightarrow K^+ Y N}(\sqrt{s}, \mathbf{p}_{K^+})/d\mathbf{p}_{K^+}$ and $E_{K^-} d\sigma_{pN \rightarrow NN K K^-}(\sqrt{s}, \mathbf{p}_{K^-})/d\mathbf{p}_{K^-}$, $E_{K^-} d\sigma_{pn \rightarrow dK^+ K^-}(\sqrt{s}, \mathbf{p}_{K^-})/d\mathbf{p}_{K^-}$ for K^+ and K^- production in the reactions (1), (2) and (3), (4), entering into eqs. (5), (9) and (6), (10), respectively. Following refs. [17, 22, 23], we assume that these cross sections are equivalent to the respective on-shell cross sections calculated for the off-shell kinematics of the elementary processes (1)–(4) at the same collision energy \sqrt{s} .

In our approach the invariant inclusive cross sections for K^+ production in the reactions (1), (2) have been described by the three-body phase-space calculations corrected for the FSI effects between the hyperons and nucleons³ following the corresponding Watson-Migdal theory [38, 39] and adopting the inverse Jost-function approximation [23] for the FSI amplitude M_{FSI}^{YN} :

$$E_{K^+} \frac{d\sigma_{pN \rightarrow K^+ Y N}(\sqrt{s}, \mathbf{p}_{K^+})}{d\mathbf{p}_{K^+}} = \frac{\pi}{4} \frac{\sigma_{pN \rightarrow K^+ Y N}(\sqrt{s})}{I_3(s, m_K, m_Y, m_N, F_{\text{FSI}}^{YN})} \times \quad (14)$$

$$\times \frac{\lambda(s_{YN}, m_Y^2, m_N^2)}{s_{YN}} F_{\text{FSI}}^{YN}(s_{YN}),$$

where

$$I_3(s, m_K, m_Y, m_N, F_{\text{FSI}}^{YN}) = \left(\frac{\pi}{2}\right)^2 \int_{(m_Y+m_N)^2}^{(\sqrt{s}-m_K)^2} \frac{\lambda(s_{YN}, m_Y^2, m_N^2)}{s_{YN}} \times \quad (15)$$

$$\times \frac{\lambda(s, s_{YN}, m_K^2)}{s} F_{\text{FSI}}^{YN}(s_{YN}) ds_{YN},$$

$$\lambda(x, y, z) = \sqrt{[x - (\sqrt{y} + \sqrt{z})^2][x - (\sqrt{y} - \sqrt{z})^2]}, \quad (16)$$

$$s_{YN} = s + m_K^2 - 2(E_0 + E_t)E_{K^+} + 2(\mathbf{p}_0 + \mathbf{p}_t)\mathbf{p}_{K^+}, \quad (17)$$

$$E_0 = \sqrt{\mathbf{p}_0^2 + m_N^2}, \quad E_{K^+} = \sqrt{\mathbf{p}_{K^+}^2 + m_K^2}. \quad (18)$$

Here, $\sigma_{pN \rightarrow K^+ Y N}$ are the total cross sections for K^+ production in reactions (1), (2) taken from [13]; m_K and m_Y are the masses in free space of a kaon and a Y hyperon (Λ or Σ), respectively; F_{FSI}^{YN} is the so-called YN -FSI enhancement factor. This factor is given by [23]:

$$F_{\text{FSI}}^{YN}(s_{YN}) = \left| M_{\text{FSI}}^{YN}(q_{YN}) \right|^2 = \frac{q_{YN}^2 + \alpha_{YN}^2}{q_{YN}^2 + \beta_{YN}^2} \quad (19)$$

and

$$q_{YN} = \frac{1}{2\sqrt{s_{YN}}} \lambda(s_{YN}, m_Y^2, m_N^2). \quad (20)$$

The values of parameters $\alpha_{\Lambda p}=255.55$ MeV/c and $\beta_{\Lambda p}=-83.38$ MeV/c were calculated taking into account average S -wave Λp scattering length \bar{a} and effective range \bar{r} from [40].

Further, taking into consideration the main ⁴ FSI effects among the final nucleons ⁵ participating in the primary proton-induced reaction channel $pN \rightarrow NN K K^-$ on the same footing as that adopted in calculating the K^+ creation cross sections (14) from the elementary processes (1), (2)

³The validity of the incorporation of the elementary FSI effects into the analysis of pA reactions is an open question. Since in the subthreshold and near-threshold energy region the outgoing particles are mainly emitted in the forward directions close to each other with small relative momenta and their momenta relative to the target system essentially greater than the Fermi momentum, one may hope that the bare FSI is not drastically suppressed in nuclei. Below we present the results of the calculations with and without including FSI effects.

⁴As is well known, the KN interaction is rather weak compared to the strong NN interaction.

⁵Protons in the exit channel in line with the assumption that the K^- meson production cross sections in pp and pn interactions are the same.

as well as following the four-body phase-space model, we can represent the invariant inclusive cross section for K^- production in this channel as follows (see, also, [23]):

$$E_{K^-} \frac{d\sigma_{pN \rightarrow NNKK^-}(\sqrt{s}, \mathbf{p}_{K^-})}{d\mathbf{p}_{K^-}} = \sigma_{pN \rightarrow NNKK^-}(\sqrt{s}) f_4^{\text{FSI}}(s, \mathbf{p}_{K^-}), \quad (21)$$

where

$$f_4^{\text{FSI}}(s, \mathbf{p}_{K^-}) = I_3(s_{NNK}, m_K, m_N, m_N, F_{\text{FSI}}^{NN}) / [2I_4(s, m_K, m_K, m_N, m_N, F_{\text{FSI}}^{NN})], \quad (22)$$

$$I_4(s, m_K, m_K, m_N, m_N, F_{\text{FSI}}^{NN}) = \left(\frac{\pi}{2}\right) \int_{4m_N^2}^{(\sqrt{s}-2m_K)^2} \frac{\lambda(s_{NN}, m_N^2, m_N^2)}{s_{NN}} F_{\text{FSI}}^{NN}(s_{NN}) \times \quad (23)$$

$$\times I_3(s, m_K, \sqrt{s_{NN}}, m_K, F_{\text{FSI}}^{NN} = 1) ds_{NN},$$

$$s_{NNK} = s + m_K^2 - 2(E_0 + E_t)E_{K^-} + 2(\mathbf{p}_0 + \mathbf{p}_t)\mathbf{p}_{K^-} \quad (24)$$

and

$$E_{K^-} = \sqrt{\mathbf{p}_{K^-}^2 + m_K^2}. \quad (25)$$

Here, $\sigma_{pN \rightarrow NNKK^-}$ is the total cross section for the nonresonant (non- ϕ) K^- production in reaction (3). The NN -FSI-modified three-body phase-space volume $I_3(s_{NNK}, m_K, m_N, m_N, F_{\text{FSI}}^{NN})$ and the NN -FSI enhancement factor F_{FSI}^{NN} , appearing in (22), (23), are described by the formulas (15), (19), (20), respectively, in which one has to make the following substitutions: $s \rightarrow s_{NNK}$, $Y \rightarrow N$. The parameters α_{NN} and β_{NN} , which govern the factor F_{FSI}^{NN} , are specified as $\alpha_{NN}=164.3$ MeV/c and $\beta_{NN}=-21.9$ MeV/c.

For the free total cross section $\sigma_{pN \rightarrow NNKK^-}$ we have used the following parametrization:

$$\sigma_{pN \rightarrow NNKK^-}(\sqrt{s}) = \begin{cases} 70 \left(1 - \frac{s_{th}}{s}\right)^{2.5} [\mu\text{b}] & \text{for } 0 < \sqrt{s} - \sqrt{s_{th}} \leq 0.114 \text{ GeV,} \\ 270 \left(1 - \frac{s_{th}}{s}\right)^3 \left(\frac{s_{th}}{s}\right)^{0.8} [\mu\text{b}] & \text{for } \sqrt{s} - \sqrt{s_{th}} > 0.114 \text{ GeV,} \end{cases} \quad (26)$$

where $\sqrt{s_{th}} = 2(m_N + m_K)$ is the threshold energy for the $pN \rightarrow NNKK^-$ reaction. Its first low-excess energy part accounts for the world near-threshold experimental data for the total cross section for the production of the non- ϕ component in the $pp \rightarrow ppK^+K^-$ reaction reported in [29]. The second high-excess energy part of (26) represents the respective parametrization of the calculated exclusive total cross section of antikaon production in nucleon–nucleon interaction within the pion and kaon exchange model [41], that has been reduced by the factor of about 1.1 to match the first one at 114 MeV excess energy.

Finally, neglecting the weak final-state interaction between K^+ meson and deuteron, produced in the reaction (4) [31, 42], as well as using the pure three-body phase-space model, we can readily get the following expression for the invariant inclusive cross section for nonresonant K^- creation in this reaction (cf. eqs. (14), (15)):

$$E_{K^-} \frac{d\sigma_{pn \rightarrow dK^+K^-}(\sqrt{s}, \mathbf{p}_{K^-})}{d\mathbf{p}_{K^-}} = \frac{\pi}{4} \frac{\sigma_{pn \rightarrow dK^+K^-}(\sqrt{s})}{I_3(s, m_K, m_d, m_K)} \times \quad (27)$$

$$\times \frac{\lambda(s_{Kd}, m_K^2, m_d^2)}{s_{Kd}},$$

where

$$I_3(s, m_K, m_d, m_K) = \left(\frac{\pi}{2}\right)^2 \int_{(m_d+m_K)^2}^{(\sqrt{s}-m_K)^2} \frac{\lambda(s_{Kd}, m_d^2, m_K^2)}{s_{Kd}} \times \quad (28)$$

$$\times \frac{\lambda(s, s_{Kd}, m_K^2)}{s} ds_{Kd},$$

$$s_{Kd} = s + m_K^2 - 2(E_0 + E_t)E_{K^-} + 2(\mathbf{p}_0 + \mathbf{p}_t)\mathbf{p}_{K^-}. \quad (29)$$

Here, $\sigma_{pn \rightarrow dK^+K^-}$ is the total cross section for the non- ϕ component of the $pn \rightarrow dK^+K^-$ reaction; m_d is the mass of a deuteron. The authors of [31] have fitted their own experimental data on the total cross section $\sigma_{pn \rightarrow dK^+K^-}$ close to threshold by the following expression:

$$\sigma_{pn \rightarrow dK^+K^-}(\sqrt{s}) = \frac{1}{4}(\sigma_0 + \sigma_1), \quad (30)$$

$$\sigma_0 = A_0\epsilon^2/D, \quad \sigma_1 = A_1\epsilon^3(D + \frac{1}{2}\epsilon/\epsilon^*)/D^2, \quad D = (1 + \sqrt{1 + \epsilon/\epsilon^*})^2, \quad (31)$$

where $\epsilon = \sqrt{s} - (m_d + 2m_K)$, $\epsilon^* = 20$ MeV, $A_0 = 127 \mu\text{b}/\text{GeV}^2$, and $A_1 = 1800 \mu\text{b}/\text{GeV}^3$.

3.2. Two-step K^+ and K^- production mechanisms

At the bombarding energies of our interest (≤ 2.4 GeV) the following two-step K^+ and K^- production processes with a pion and a ϕ -meson in an intermediate states can contribute to the kaon and antikaon production in pA interactions [12, 13, 22, 30, 37]⁶:

$$p + N_1 \rightarrow \pi + X, \quad (32)$$

$$\pi + N_2 \rightarrow K^+ + \Lambda, \quad (33)$$

$$\pi + N_2 \rightarrow K^+ + \Sigma; \quad (34)$$

$$\pi + N_2 \rightarrow N + K + K^-, \quad (35)$$

$$p + N \rightarrow p + N + \phi, \quad (36)$$

$$p + n \rightarrow d + \phi, \quad (37)$$

$$\phi \rightarrow K^+ + K^-. \quad (38)$$

The K^+ and K^- production cross sections for pA interactions at small laboratory angles from the secondary pion-induced reaction channels (33), (34) and (35) can be represented as follows [12, 17, 22]:

$$E_{K^+} \frac{d\sigma_{pA \rightarrow K^+X}^{(\text{sec})}(\mathbf{p}_0)}{d\mathbf{p}_{K^+}} = \frac{I_{K^+}^{(\text{sec})}[A]}{I_\pi[A]} \sum_{\pi=\pi^+, \pi^0, \pi^-} \sum_{Y=\Lambda, \Sigma, 4\pi} \int d\Omega_\pi \int_{p_\pi^{\text{abs},+}}^{p_\pi^{\text{lim}}(\vartheta_\pi)} p_\pi^2 dp_\pi \frac{d\sigma_{pA \rightarrow \pi X}^{(\text{prim})}(\mathbf{p}_0)}{d\mathbf{p}_\pi} \times \quad (39)$$

$$\times \left[\frac{Z}{A} \left\langle E_{K^+} \frac{d\sigma_{\pi p \rightarrow K^+Y}(\mathbf{p}_\pi, \mathbf{p}_{K^+})}{d\mathbf{p}_{K^+}} \right\rangle + \frac{N}{A} \left\langle E_{K^+} \frac{d\sigma_{\pi n \rightarrow K^+Y}(\mathbf{p}_\pi, \mathbf{p}_{K^+})}{d\mathbf{p}_{K^+}} \right\rangle \right],$$

$$E_{K^-} \frac{d\sigma_{pA \rightarrow K^-X}^{(\text{sec})}(\mathbf{p}_0)}{d\mathbf{p}_{K^-}} = \frac{I_{K^-}^{(\text{sec})}[A]}{I_\pi[A]} \sum_{\pi=\pi^+, \pi^0, \pi^-} \int d\Omega_\pi \int_{p_\pi^{\text{abs},-}}^{p_\pi^{\text{lim}}(\vartheta_\pi)} p_\pi^2 dp_\pi \frac{d\sigma_{pA \rightarrow \pi X}^{(\text{prim})}(\mathbf{p}_0)}{d\mathbf{p}_\pi} \times \quad (40)$$

⁶It should be pointed out that in the intermediate pion energy region of interest the K^- mesons can be produced in πN collisions also by the decay of the ϕ meson as an intermediate state in the process $\pi N \rightarrow \phi N$, $\phi \rightarrow K^+K^-$. However, in view of the fact that the resonant (ϕ meson) to total K^- production cross section ratio for example in π^-p reactions at pion energies of interest, as showed our estimates using the results given in [43, 44], is rather small (about 0.1), it is natural to assume, calculating the K^- yields in pA reactions from the secondary channel (35), that the antikaons are produced directly in this channel.

$$\times \left[\frac{Z}{A} \left\langle E_{K^-} \frac{d\sigma_{\pi p \rightarrow NKK^-}(\mathbf{p}_\pi, \mathbf{p}_{K^-})}{d\mathbf{p}_{K^-}} \right\rangle + \frac{N}{A} \left\langle E_{K^-} \frac{d\sigma_{\pi n \rightarrow NKK^-}(\mathbf{p}_\pi, \mathbf{p}_{K^-})}{d\mathbf{p}_{K^-}} \right\rangle \right],$$

where

$$I_h^{(\text{sec})}[A] = 2\pi A^2 \int_0^{+\infty} r_\perp dr_\perp \int_{-\infty}^{+\infty} dz \rho(\sqrt{r_\perp^2 + z^2}) \int_0^{+\infty} dl \rho(\sqrt{r_\perp^2 + (z+l)^2}) \times \quad (41)$$

$$\times \exp \left[-\sigma_{pN}^{\text{in}} A \int_{-\infty}^z \rho(\sqrt{r_\perp^2 + x^2}) dx - \sigma_{\pi N}^{\text{tot}} A \int_z^{z+l} \rho(\sqrt{r_\perp^2 + x^2}) dx \right] \times$$

$$\times \exp \left[-\sigma_{hN}^{\text{tot}}(p_h) A \int_{z+l}^{+\infty} \rho(\sqrt{r_\perp^2 + x^2}) dx \right],$$

$$\left\langle E_{K^+} \frac{d\sigma_{\pi N \rightarrow K^+Y}(\mathbf{p}_\pi, \mathbf{p}_{K^+})}{d\mathbf{p}_{K^+}} \right\rangle = \int n(\mathbf{p}_t) d\mathbf{p}_t \left[E_{K^+} \frac{d\sigma_{\pi N \rightarrow K^+Y}(\sqrt{s_1}, \mathbf{p}_{K^+})}{d\mathbf{p}_{K^+}} \right], \quad (42)$$

$$\left\langle E_{K^-} \frac{d\sigma_{\pi N \rightarrow NKK^-}(\mathbf{p}_\pi, \mathbf{p}_{K^-})}{d\mathbf{p}_{K^-}} \right\rangle = \int n(\mathbf{p}_t) d\mathbf{p}_t \left[E_{K^-} \frac{d\sigma_{\pi N \rightarrow NKK^-}(\sqrt{s_1}, \mathbf{p}_{K^-})}{d\mathbf{p}_{K^-}} \right]; \quad (43)$$

$$s_1 = (E_\pi + E_t)^2 - (p_\pi \boldsymbol{\Omega}_0 + \mathbf{p}_t)^2, \quad (44)$$

$$p_\pi^{\text{lim}}(\vartheta_\pi) = \frac{\beta_A p_0 \cos \vartheta_\pi + (E_0 + M_A) \sqrt{\beta_A^2 - 4m_\pi^2 (s_A + p_0^2 \sin^2 \vartheta_\pi)}}{2(s_A + p_0^2 \sin^2 \vartheta_\pi)}, \quad (45)$$

$$\beta_A = s_A + m_\pi^2 - M_{A+1}^2, \quad s_A = (E_0 + M_A)^2 - p_0^2, \quad (46)$$

$$\cos \vartheta_\pi = \boldsymbol{\Omega}_0 \boldsymbol{\Omega}_\pi, \quad \boldsymbol{\Omega}_0 = \mathbf{p}_0/p_0, \quad \boldsymbol{\Omega}_\pi = \mathbf{p}_\pi/p_\pi. \quad (47)$$

Here, $d\sigma_{pA \rightarrow \pi X}^{(\text{prim})}(\mathbf{p}_0)/d\mathbf{p}_\pi$ are the inclusive differential cross sections for pion production on nuclei at small laboratory angles and for high momenta from the primary proton-induced reaction channel (32); $E_{K^+} d\sigma_{\pi N \rightarrow K^+Y}(\sqrt{s_1}, \mathbf{p}_{K^+})/d\mathbf{p}_{K^+}$ and $E_{K^-} d\sigma_{\pi N \rightarrow NKK^-}(\sqrt{s_1}, \mathbf{p}_{K^-})/d\mathbf{p}_{K^-}$ are the free inclusive invariant cross sections for K^+ and K^- production via the subprocesses (33), (34) and (35) calculated for the off-shell kinematics of these subprocesses at the πN center-of-mass energy $\sqrt{s_1}$; $\sigma_{\pi N}^{\text{tot}}$ is the total cross section of the free πN interaction⁷; \mathbf{p}_π and E_π are the momentum and total energy of a pion (which is assumed to be on-shell); m_π is the rest mass of a pion; $p_\pi^{\text{abs},+(-)}$ is the absolute threshold momentum for kaon (antikaon) production on the residual nucleus by an intermediate pion; $p_\pi^{\text{lim}}(\vartheta_\pi)$ is the kinematical limit for pion production at the lab angle ϑ_π from proton-nucleus collisions; M_A and M_{A+1} are the ground state masses of the initial target nucleus and nucleus containing $A+1$ nucleons. The quantity $I_\pi[A]$, entering into (39), (40), is defined above by eq. (7) in which one has to make the substitution $h \rightarrow \pi$.

The elementary K^+ and K^- production reactions $\pi^+ n \rightarrow K^+ \Lambda$, $\pi^0 p \rightarrow K^+ \Lambda$, $\pi^+ p \rightarrow K^+ \Sigma^+$, $\pi^+ n \rightarrow K^+ \Sigma^0$, $\pi^0 p \rightarrow K^+ \Sigma^0$, $\pi^0 n \rightarrow K^+ \Sigma^-$, $\pi^- p \rightarrow K^+ \Sigma^-$ and $\pi^+ n \rightarrow pK^+ K^-$, $\pi^0 p \rightarrow pK^+ K^-$, $\pi^0 n \rightarrow nK^+ K^-$, $\pi^0 n \rightarrow pK^0 K^-$, $\pi^- p \rightarrow nK^+ K^-$, $\pi^- p \rightarrow pK^0 K^-$, $\pi^- n \rightarrow nK^0 K^-$ have been included in our calculations of the K^+ and K^- production on nuclei. In them, the differential cross sections for kaon and antikaon creation in these reactions have been computed following strictly the approach [12, 22].

Another very important ingredients for the calculation of the K^+ and K^- production cross sections in proton-nucleus reactions from pion-induced reaction channels (33), (34) and (35)—the high-momentum parts of the differential cross sections for pion production on nuclei at small lab angles from the primary process (32)—for ^9Be and ^{63}Cu target nuclei were taken from [17, 22].

⁷We use in the following calculations $\sigma_{\pi N}^{\text{tot}} = 35$ mb for all pion momenta [22].

Now consider the K^- production in pA reactions via the phi production/decay sequences (36)–(38). Taking into account the fact that the most of ϕ mesons, which are responsible for the sub-threshold antikaon production in pA collisions for kinematics of our experiment, decay into K^+ and K^- mesons essentially outside the target nuclei of interest [37, 45] as well as using the results given in [17, 37, 46], we get the following expression for the K^- production cross section for pA interactions from these sequences:

$$E_{K^-} \frac{d\sigma_{pA \rightarrow \phi X, \phi \rightarrow K^+ K^-}(\mathbf{p}_0)}{d\mathbf{p}_{K^-}} = I_\phi[A] \left(\frac{M_\phi}{m_{K^-}} \right)^2 BR_{\phi \rightarrow K^+ K^-}(M_\phi) \int \frac{d\Omega_\phi^*}{4\pi} \times \quad (48)$$

$$\times \left[\frac{Z}{A} \left\langle E_\phi \frac{d\sigma_{pp \rightarrow pp\phi}(\mathbf{p}_0, \mathbf{p}_\phi)}{d\mathbf{p}_\phi} \right\rangle + \frac{N}{A} \left\langle E_\phi \frac{d\sigma_{pn \rightarrow pn\phi}(\mathbf{p}_0, \mathbf{p}_\phi)}{d\mathbf{p}_\phi} \right\rangle + \frac{N}{A} \left\langle E_\phi \frac{d\sigma_{pn \rightarrow d\phi}(\mathbf{p}_0, \mathbf{p}_\phi)}{d\mathbf{p}_\phi} \right\rangle \right],$$

where

$$\left\langle E_\phi \frac{d\sigma_{pN \rightarrow pN\phi(pn \rightarrow d\phi)}(\mathbf{p}_0, \mathbf{p}_\phi)}{d\mathbf{p}_\phi} \right\rangle = \int n(\mathbf{p}_t) d\mathbf{p}_t \left[E_\phi \frac{d\sigma_{pN \rightarrow pN\phi(pn \rightarrow d\phi)}(\sqrt{s}, M_\phi, \mathbf{p}_\phi)}{d\mathbf{p}_\phi} \right]. \quad (49)$$

Here, $E_\phi d\sigma_{pN \rightarrow pN\phi}(\sqrt{s}, M_\phi, \mathbf{p}_\phi)/d\mathbf{p}_\phi$ and $E_\phi d\sigma_{pn \rightarrow d\phi}(\sqrt{s}, M_\phi, \mathbf{p}_\phi)/d\mathbf{p}_\phi$ are the off-shell differential cross sections for ϕ production in reactions (36) and (37), respectively, at the pN center-of-mass energy \sqrt{s} and at its pole mass ⁸ M_ϕ ; \mathbf{p}_ϕ and E_ϕ are the momentum and total energy of a ϕ meson ($E_\phi = \sqrt{\mathbf{p}_\phi^2 + M_\phi^2}$); Ω_ϕ^* is its solid angle in the rest frame of the detected antikaon. The quantity $I_\phi[A]$ in (48) is defined above by eq. (7) in which one has to make the substitution $h \rightarrow \phi$. For the total ϕN cross section $\sigma_{\phi N}^{\text{tot}}$ appearing in this quantity we have used the value of 8.3 mb [47].

In our calculations of the K^- meson production on nuclei the differential cross sections $E_\phi d\sigma_{pN \rightarrow pN\phi}(\sqrt{s}, M_\phi, \mathbf{p}_\phi)/d\mathbf{p}_\phi$ and $E_\phi d\sigma_{pn \rightarrow d\phi}(\sqrt{s}, M_\phi, \mathbf{p}_\phi)/d\mathbf{p}_\phi$, entering into eqs. (48), (49), have been computed within the approach [45]. In doing so, the corresponding parametrization for the free total cross section $\sigma_{pp \rightarrow pp\phi}(\sqrt{s})$ of the $pp \rightarrow pp\phi$ reaction presented in [45] has been reduced by the factor of 1.33 in line with the new set of data [29] for this reaction in the threshold region and the cross section ratio $\sigma_{pn \rightarrow pn\phi}/\sigma_{pp \rightarrow pp\phi}$ has been employed in the excess-energy-dependent form from [48].

3.3. Comparison with the experimental data

At first, we will concentrate on the results of our calculations for the production of K^+ mesons from $p\text{Be}$, $p\text{C}$ and $p\text{Cu}$ reactions at the various bombarding energies.

Figures 2 and 3 show a comparison of the experimental data from the present experiment for the invariant differential cross sections for the production of K^+ mesons, respectively, in $p+\text{Be}$ and $p+\text{Cu}$ interactions at the laboratory angle of 10.5° and for the initial proton energy of 1.7 GeV with the calculated ones according to (5), (39). It is seen that the pion-induced K^+ creation processes (33), (34) do not dominate in the kaon production in $p^9\text{Be}$ collisions at all kaon momenta and the main contribution to the kaon yield here comes from the direct K^+ production mechanism in both considered scenarios with and without including the FSI effects between the hyperons and nucleons produced via this mechanism. In the case of $p^{63}\text{Cu}$ interactions the direct mechanism clearly dominates the K^+ production only at high kaon momenta ⁹ (at $p_{K^+} \geq 0.8$ GeV/c ¹⁰). It is also seen that the inclusion of the YN -FSI effects (dash-dotted lines in Figs. 2 and 3) enhances the

⁸Since a ϕ -meson is a narrow resonance.

⁹This is consistent with the previous findings of [5, 13] about the role played by the direct K^+ production mechanism in the "hard" kaon creation in pA reactions and in line with the BUU transport calculation [9].

¹⁰It should be noted that for kinematical conditions of our experiment the data points in Figs. 2 and 3 which correspond to the laboratory kaon momenta $p_{K^+} \geq 0.8$ GeV/c are the subthreshold data points.

kaon spectra from the one-step processes (1), (2) at these momenta by a factor of about 2. As a result, our overall calculations (the sum of contributions both from the one-step (1), (2) and from the two-step (33), (34) reaction channels, solid lines) reproduce well the measured K^+ invariant differential cross section in the case of ${}^9\text{Be}$ target nucleus. As for the ${}^{63}\text{Cu}$ target nucleus, while our full model calculations with including the YN -FSI effects reproduce quite good the shape of the measured kaon spectrum, they nevertheless overestimate the strength of it by a factor of around 2. The calculations without including of the FSI effects provide better description of the data obtained on ${}^{63}\text{Cu}$ target.

In Figures 4 and 5 we show a comparison of the results of our calculations for the double differential K^+ spectra at an angle of 4° for $p+{}^{12}\text{C}$ collisions at beam energies of 1.5 and 2.0 GeV with the experimental data from [8] taken by the ANKE-at-COSY Collaboration at forward laboratory angles $\leq 12^\circ$. These figures demonstrate that the proton-induced reaction channels (1), (2) dominate the K^+ production also in the case of ${}^{12}\text{C}$ target nucleus for both bombarding energies under consideration. It can be also seen from them that while the data at 2.0 GeV incident energy are rather well described by the overall calculations when taking the YN -FSI effects into account (solid line in Fig. 5), the spectrum at 1.5 GeV beam energy is underestimated largely in the momentum range above 300 MeV/c for these effects included. This is possible tied to the fact that two different normalization methods have been used for the data sets at 2.0 and 1.5 GeV beam energies.

Reasonable description of the kaon spectra in the wide momentum range at different production angles (Figs. 2–5) offers the possibility to compare the data [8] with those obtained in this experiment in spite of the kinematical conditions of the ANKE measurements are not identical to those of the present experiment. The double differential cross sections measured by us at initial proton energy $\epsilon_0=1.7$ GeV¹¹ lie within the confines of the solid curves in Figs. 4, 5 referring to $\epsilon_0=1.5$ GeV and $\epsilon_0=2$ GeV. Moreover, the target mass dependences - presented in the form $\sigma \sim A^\alpha$ - are quite similar. The value of cross section ratio Au/C measured at 1.75 GeV beam energy (Table 8 in [8])¹² corresponds to the magnitude of $\alpha=0.47\pm 0.04$ for maximal kaon momentum of 0.596 GeV/c, while the Cu/Be ratio (see Table 1) yields $\alpha=0.48\pm 0.09$ for minimal kaon momentum of 0.675 GeV/c. Thus, one can conclude that the results of two measurements are compatible.

The data from the present experiment for the invariant inclusive cross sections for the production of K^- mesons at an angle of 10.5° in the interaction of 2.25 and 2.4 GeV protons with the ${}^9\text{Be}$ nuclei are displayed, respectively, in Figs. 6 and 7 in comparison to the calculated ones by (6), (40), (48). The same as in Fig. 7, but for the interaction of 2.4 GeV protons with the ${}^{63}\text{Cu}$ nuclei is given in Fig. 8. It is seen that the contributions from the resonant channels $pN \rightarrow pN\phi$, $pn \rightarrow d\phi$, $\phi \rightarrow K^+K^-$ are small at antikaon momenta above 1.0 GeV/c¹³, whereas at lower K^- momenta their role is essentially more important. Thus, at these momenta the contributions to the K^- production from the production/decay sequence $pN \rightarrow pN\phi$, $\phi \rightarrow K^+K^-$ and pion-induced reaction channel $\pi N \rightarrow NK^-$ and from primary non-resonant proton-nucleon production process $pN \rightarrow NNKK^-$ and resonant channel $pn \rightarrow d\phi$, $\phi \rightarrow K^+K^-$ are comparable. It is also clearly seen that the main contributions to the subthreshold antikaon production in $p+{}^9\text{Be}$, $p+{}^{63}\text{Cu}$ interactions at low antikaon momenta ($p_{K^-} \leq 0.6$ GeV/c) come from the secondary K^- production processes $\pi N \rightarrow NK^-$ and $pN \rightarrow pN\phi$, $\phi \rightarrow K^+K^-$, whereas at high antikaon momenta ($p_{K^-} \geq 1.0$ GeV/c) the primary non-resonant (non- ϕ) proton-induced reaction channels $pn \rightarrow dK^+K^-$ and $pN \rightarrow NNKK^-$ are dominant. It should be pointed out that their dominance here for the ${}^{63}\text{Cu}$ target nucleus, contrary to the case of ${}^9\text{Be}$ nucleus, is less pronounced. The inclusion of the FSI

¹¹The absolute normalization in [8] was not established at the initial proton energy $\epsilon_0=1.75$ GeV which is close to $\epsilon_0=1.7$ GeV in the present study.

¹²The cross section ratios do not depend on the normalization.

¹³In particular, this is in line with the conclusion about the relative role of the phi production/decay process $pN \rightarrow pN\phi$, $\phi \rightarrow K^+K^-$ in "hard" antikaon production also from $p\text{Be}$ and $p\text{Cu}$ reactions inferred in [17].

effects among the outgoing nucleons participating in the non-resonant $pN \rightarrow NNKK^-$ channel (dash-dotted lines in Figs. 6–8) enhances the high-momentum parts ($p_{K^-} \geq 1.0$ GeV/c) of the antikaon spectra from this channel by a factor of about 1.2–2.0 and practically does not affect their low-momentum parts ($p_{K^-} \leq 0.6$ GeV/c). As a result, our full calculations (solid lines in Figs. 6–8) reproduce quite well the measured K^- invariant inclusive cross sections for both target nuclei. The important point is that to reproduce the high-momentum tails of the antikaon spectra it was also significant to take into consideration the contribution from the new K^- production channel non- ϕ $pn \rightarrow dK^+K^-$.

Good agreement of the measured antikaon spectra with our calculations evidences for weak influence of the in-medium kaon and antikaon potentials on the K^- yields from the reactions with KK^- in the final state $pN \rightarrow NNKK^-$, $\pi N \rightarrow NKK^-$, $pn \rightarrow dKK^-$, $pN \rightarrow pN\phi$, $pn \rightarrow d\phi$, $\phi \rightarrow K^+K^-$. This observation is in line with the analysis [22, 23], based on the spectral function approach, where it has been shown that the simultaneous application of the density-dependent weak repulsive K^+ and relatively deep attractive K^- nuclear potentials of +22 MeV and -126 MeV at saturation density remains unaffected antikaon spectra with momentum of more than 0.8 GeV/c compared to the case with zero kaon and antikaon nuclear mean fields. Similar cancellation has been found in [17] where reasonable description of the K^- excitation function for the pBe and pCu reactions measured for K^- momentum of 1.28 GeV/c at beam energy <3 GeV was reached in the frame of the folding model with nucleon momentum distribution (13) assuming vacuum K^+ , K^- masses as well as kaon and antikaon masses modified by their potentials. These arguments are not valid for the reactions with the K^- alone in the final state. The impact of the antikaon self-energy on the K^- yield from $YN \rightarrow NNK^-$ reaction can be essential.

The importance of the strangeness exchange processes $pN \rightarrow K^+YN$; $YN \rightarrow NNK^-$, $Y\pi \rightarrow NK^-$ for antikaon production in pA reactions was pointed out in [18, 21]. According to the BUU calculation the contribution of the strangeness exchange reactions in the cross sections for antikaon production at 40–56⁰ by 2.5 GeV protons reaches to 50–60 % for heavy gold target. No significant influence is found for light carbon target. It should be pointed out that the results of such calculations are model-dependent, since the cross section of the $YN \rightarrow NNK^-$ reaction experimentally is not known. To produce K^- at the second step of the strangeness exchange process $YN \rightarrow NNK^-$ the hyperon with high momentum exceeding 1.3 GeV/c at the first step $pN \rightarrow K^+YN$ is required. All known experimental data on forward hadron production from nuclei with $A \geq 9$ evidence for strong decreasing of the cross sections with Feynman variable X_F^R (see, for instance, Fig. 1). The drop of the high-momentum parts of the π^+ and π^- spectra in the energy range from 2 to 24 GeV [17, 49, 50] as well as decrease of the antiproton spectra [14] at initial proton energies of 3–5 GeV follow the dependence $(1 - X_F^R)^\delta$ with $\delta \geq 4$. Thus, it is natural to suppose that the high-momentum part of the hyperon spectrum also follows this dependence with $\delta \geq 4$. In Fig. 9 we compare the behavior of the X_R^F as a function of $P_{t,min}$ for the present experiment and [18]. The $P_{t,min}$ is a minimal (threshold) momentum of intranuclear nucleon required for the K^- production in direct $pN \rightarrow K^-KNN$ process in the kinematics of particular experiment. The value of $P_{t,min}$ is defined by eq. 24 with $S_{NNK} = (2m_N + m_K)^2$. Experimental data obtained in [17, 18] as well as data from the present study evidence that at equal $P_{t,min}$ the double differential cross sections for the antikaon production are comparable. Fig. 9 demonstrates that the values of X_R^F calculated for the kinematical conditions of our experiment significantly exceed ones for the experiment [18]. Hence, the contribution of the $YN \rightarrow NNK^-$ channel in the kinematics of the present experiment is less than that in [18] at least by a factor of 7–10¹⁴. Our estimate shows that the contribution of strangeness exchange channel in the cross section for antikaon production on Cu target does not exceed 10–15%. Good description of the K^- data obtained on both Be and Cu nuclei (see Figs. 6, 7, 8) supports this conclusion.

¹⁴We use $\delta=3.5$ for this estimate

Taking into account the above considerations, we conclude that our model calculations support the proposed mechanisms for the subthreshold and near-threshold charged kaons production in the case of $p+{}^9\text{Be}$, $p+{}^{12}\text{C}$ and $p+{}^{63}\text{Cu}$ collisions.

4. Conclusions

In this paper we have presented the experimental data on the invariant inclusive cross sections for the production of K^+ and K^- mesons in the momentum range from 0.6 to 1.3 GeV/c at a lab angle of 10.5° in $p+\text{Be}$, $p+\text{Cu}$ interactions, respectively, at 1.7 and 2.25, 2.4 GeV beam energies. This is the first measurement of antikaon spectra in proton-induced reactions on nuclei in the subthreshold energy regime. The above experimental data as well as those from [8] for K^+ production in $p+\text{C}$ collisions at 1.5 and 2.0 GeV incident energies, obtained by the ANKE-at-COSY Collaboration, are compared to the results of calculations in the framework of an appropriate folding model for incoherent primary proton-nucleon, secondary pion-nucleon kaon and antikaon production processes and processes associated with the creation of antikaons via the decay of intermediate ϕ -mesons. The model is based on the struck target nucleon momentum distribution and on free elementary cross sections. The comparison of the data to our model calculations indicates that the proposed mechanisms for the subthreshold and near-threshold charged kaons production in pA reactions are realistic enough. It was shown for the first time that the antikaon production for the momentum $p_K < 0.8$ GeV/c is dominated by the $pN \rightarrow pN\phi$; $\phi \rightarrow K^+K^-$ channel on light ${}^9\text{Be}$ nucleus. On ${}^{63}\text{Cu}$ nucleus the main contribution to the cross section comes from this channel and $\pi N \rightarrow NKK^-$ process.

It was also shown that the strangeness exchange mechanism plays a minor role in the processes of the production of the antikaons with momentum larger than 0.6 GeV/c emitted in forward direction from proton-induced reactions. We have argued that the cross sections of the reactions with KK^- in the final state are weakly influenced by the in-medium kaon and antikaon mean fields. The performed calculations showed that accounting for the hyperon-nucleon and nucleon-nucleon FSI effects mostly results in better description of the high momentum tails of the kaon and antikaon spectra.

Acknowledgments

Two of the authors (Yu. K. and E. P.) acknowledge M. Hartmann, which has attracted our attention to the new possible K^- production channel non- ϕ $pn \rightarrow dK^+K^-$. This study was partly supported by the Russian Fund for Basic Research under grant No. 07-02-91565.

References

- [1] V. P. Koptev *et al.*, Sov. Phys. JETP **67**, 2177 (1988).
- [2] S. Schnetzer *et al.*, Phys. Rev. C **40**, 640 (1989).
- [3] M. Debowski *et al.*, Z. Phys. A **356**, 313 (1996).
- [4] A. Badala *et al.*, Phys. Rev. Lett. **80**, 4863 (1998).
- [5] A. V. Akindinov *et al.*, JETP Lett. **72**, 100 (2000).
- [6] V. Koptev *et al.*, Phys. Rev. Lett. **87**, 022301 (2001).

- [7] M. Nekipelov *et al.*, Phys. Lett. B **540**, 207 (2002).
- [8] M. Büscher *et al.*, Eur. Phys. J. A **22**, 301 (2004).
- [9] Z. Rudy *et al.*, Eur. Phys. J. A **15**, 303 (2002).
- [10] Z. Rudy *et al.*, Eur. Phys. J. A **23**, 379 (2005). Erratum *ibid.* A **24**, 159 (2005).
- [11] M. Büscher *et al.*, Phys. Rev. C **65**, 014603 (2001).
- [12] S. V. Efremov and E. Ya. Paryev, Eur. Phys. J. A **1**, 99 (1998).
- [13] E. Ya. Paryev, Eur. Phys. J. A **5**, 307 (1999).
- [14] Y. Sugaya *et al.*, Nucl. Phys. A **634**, 115 (1998).
- [15] A. A. Baldin *et al.*, JINR Rapid Communications **2(54)-92**, Dubna, p.20 (1992).
- [16] Yu. T. Kiselev (for the FHS Collab.), J. Phys. G. **25**, 381 (1999).
- [17] A. V. Akindinov *et al.*, JETP Lett. **85**, 142 (2007).
- [18] W. Scheinast *et al.*, Phys. Rev. Lett. **96**, 072301 (2006).
- [19] A. Sibirtsev *et al.*, Z. Phys. A **351**, 333 (1995).
- [20] A. Sibirtsev and W. Cassing, Nucl. Phys. A **641**, 476 (1998).
- [21] H. W. Barz and L. Naumann, Phys. Rev. C **68**, 041901 (2003).
- [22] E. Ya. Paryev, Eur. Phys. J. A **9**, 521 (2000).
- [23] E. Ya. Paryev, Eur. Phys. J. A **17**, 145 (2003); Phys. of Atom. Nucl. **65**, 1877 (2002).
- [24] A. Shor *et al.*, Nucl. Phys. A **514**, 717 (1990).
- [25] W. Cassing *et al.*, Phys. Lett. B **238**, 25 (1990).
- [26] A. Sibirtsev and M. Büscher, Z. Phys. A **347**, 191 (1994).
- [27] W. Cassing *et al.*, Z. Phys. A **349**, 77 (1994).
- [28] M. Hartmann, Yu. Kiselev *et al.*, ANKE-COSY proposal #147 (2005).
- [29] Y. Maeda *et al.*, Phys. Rev. C **77**, 015204 (2008).
- [30] Y. Maeda *et al.*, Phys. Rev. Lett. **97**, 142301 (2006).
- [31] Y. Maeda *et al.*, Phys. Rev. C **79**, 018201 (2009).
- [32] M.F.M. Lutz *et al.*, Nucl. Phys. A **808**, 124 (2008).
- [33] M. M. Firoozabadi *et al.*, Instruments and Experimental Techniques **42**, 182 (1999).
- [34] C. Amsler *et al.*, PDG, Phys. Lett. B **667**, 1 (2008).
- [35] S. V. Efremov and E. Ya. Paryev, Z. Phys. A **348**, 217 (1994).
- [36] G. Q. Li *et al.*, Nucl. Phys. A **625**, 372 (1997).

- [37] E. Ya. Paryev, Eur. Phys. J. A **23**, 453 (2005).
- [38] K. M. Watson, Phys. Rev. **88**, 1163 (1952).
- [39] A. B. Migdal, JETP **1**, 2 (1955).
- [40] J. T. Balewski *et al.*, Eur. Phys. J. A **2**, 99 (1998).
- [41] A. Sibirtsev *et al.*, Z. Phys. A **358**, 101 (1997).
- [42] A. Dzyuba *et al.*, Eur. Phys. J. A **38**, 1 (2008).
- [43] S. V. Efremov and E. Ya. Paryev, Z. Phys. A **351**, 447 (1995).
- [44] M. Döring *et al.*, nucl-th/0805.1799.
- [45] E. Ya. Paryev, Phys. At. Nucl. **71**, 1954 (2008).
- [46] Y. Nara *et al.*, Nucl. Phys. A **614**, 433 (1997).
- [47] H. Behrend *et al.*, Phys. Lett. B **56**, 408 (1975).
- [48] L. P. Kaptari and B. Kämpfer, Eur. Phys. J. A **23**, 291 (2005).
- [49] Yu. D. Bayukov *et al.*, Yadernaya Fizika **29**, 947 (1979)
- [50] T. Eichten *et al.*, Nucl. Phys. B **44**, 333 (1972).

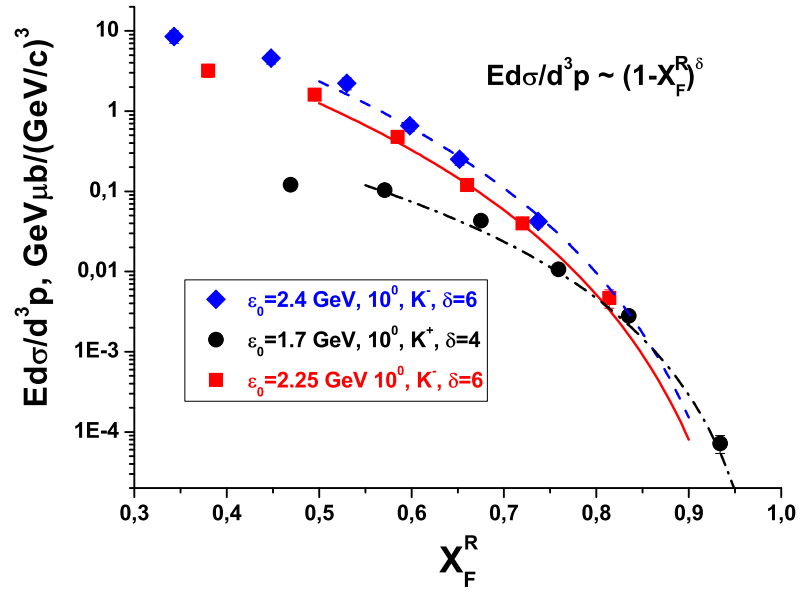


Figure 1: Invariant cross sections for the kaon and antikaon production as a function of radial Feynman variable X_F^R .

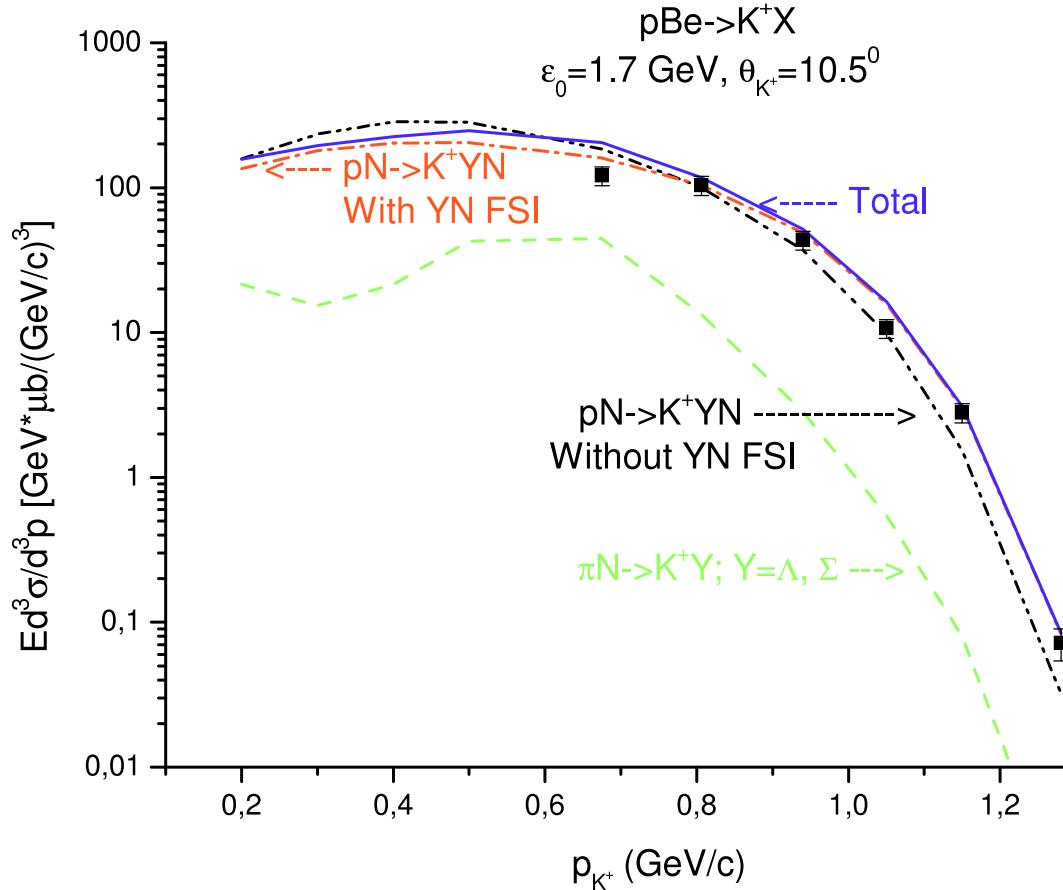


Figure 2: Invariant cross sections for the production of K^+ mesons at an angle of 10.5° in the interaction of 1.7 GeV protons with the ${}^9\text{Be}$ nuclei as functions of kaon momentum. The experimental data (full squares) are obtained at the ITEP accelerator (see Table 1). The curves are our calculation. The dashed lines with one and two dots are calculations for the primary production processes $pN \rightarrow K^+YN$; $Y = \Lambda, \Sigma$ with and without including the FSI effects among the outgoing hyperons and nucleons. The dashed line is calculation for the secondary production processes $\pi N \rightarrow K^+Y$ with an intermediate pion. The solid line is the sum of the dashed and dash-dotted lines.

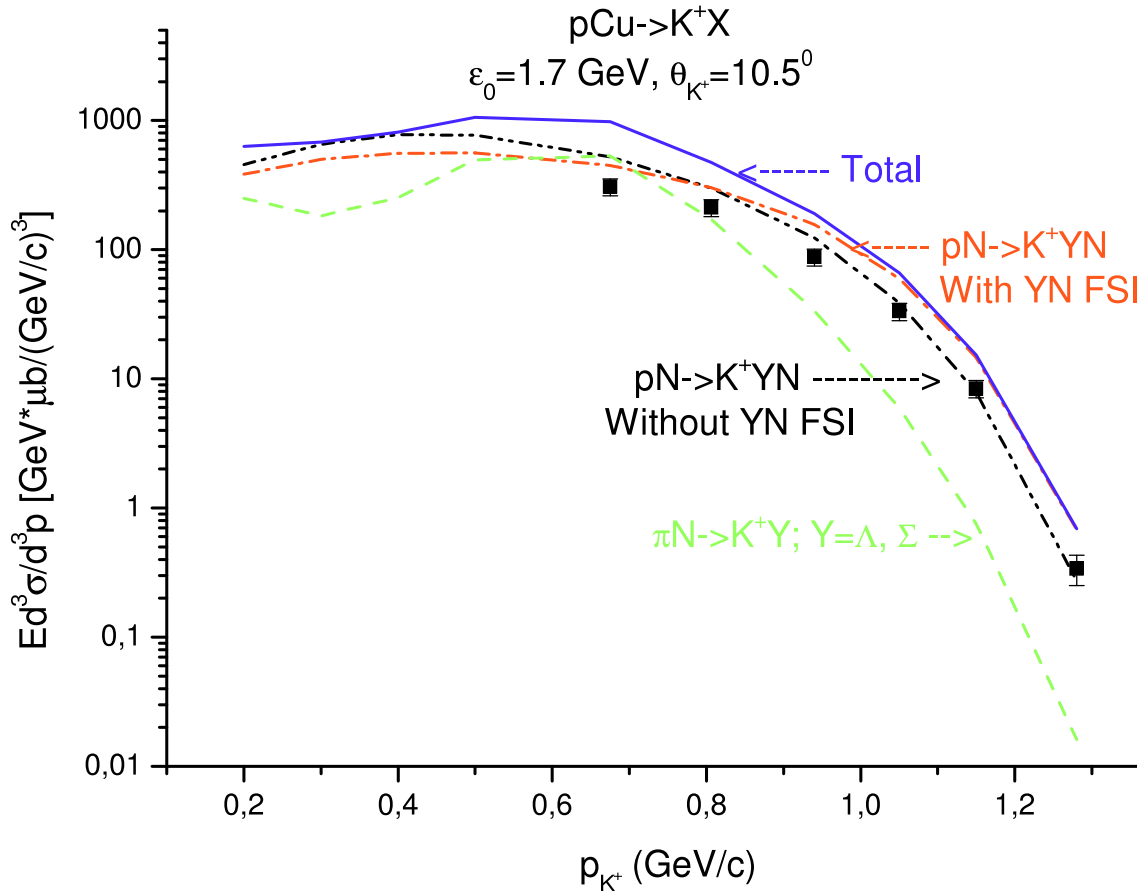


Figure 3: The same as in Fig. 2, but for the interaction of protons with the ^{63}Cu nuclei.

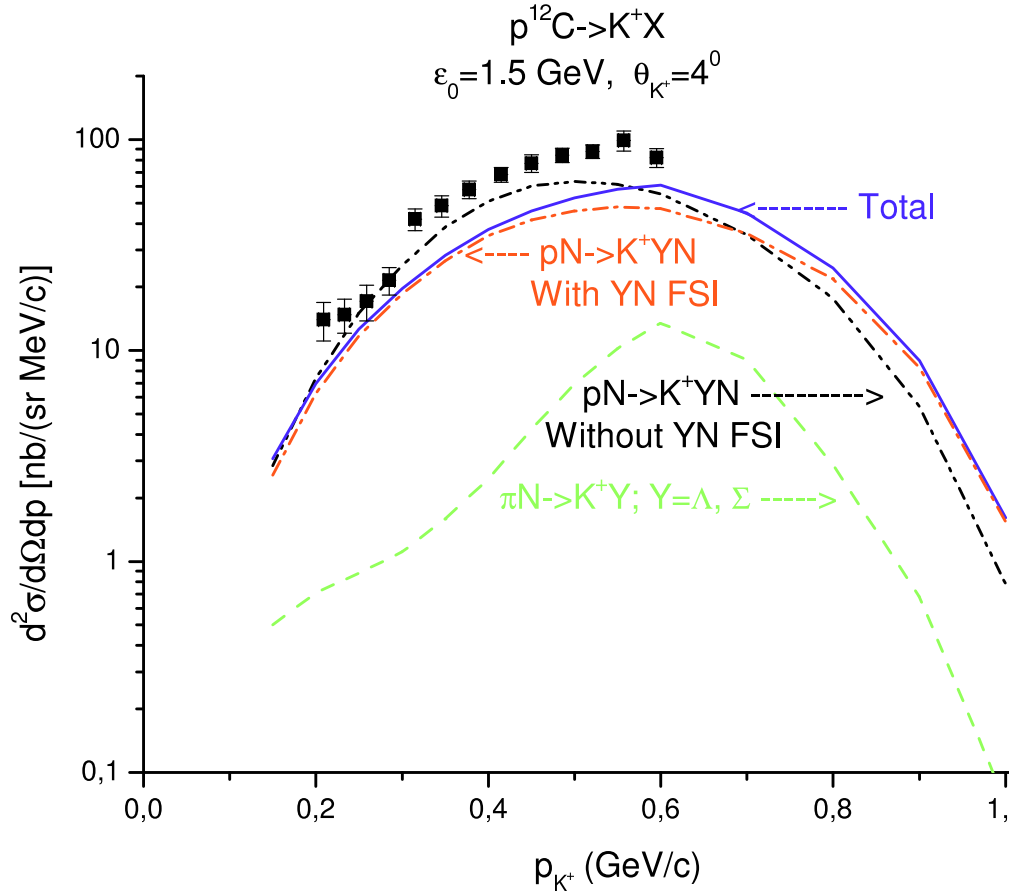


Figure 4: Double differential cross sections for the production of K^+ mesons in the interaction of 1.5 GeV protons with the ^{12}C nuclei as functions of kaon momentum. The experimental data (full squares), taken at forward laboratory angles $\leq 12^\circ$, are from [8]. The curves are our calculation at an angle of 4° . The notation of the curves is identical to that in Fig. 2.

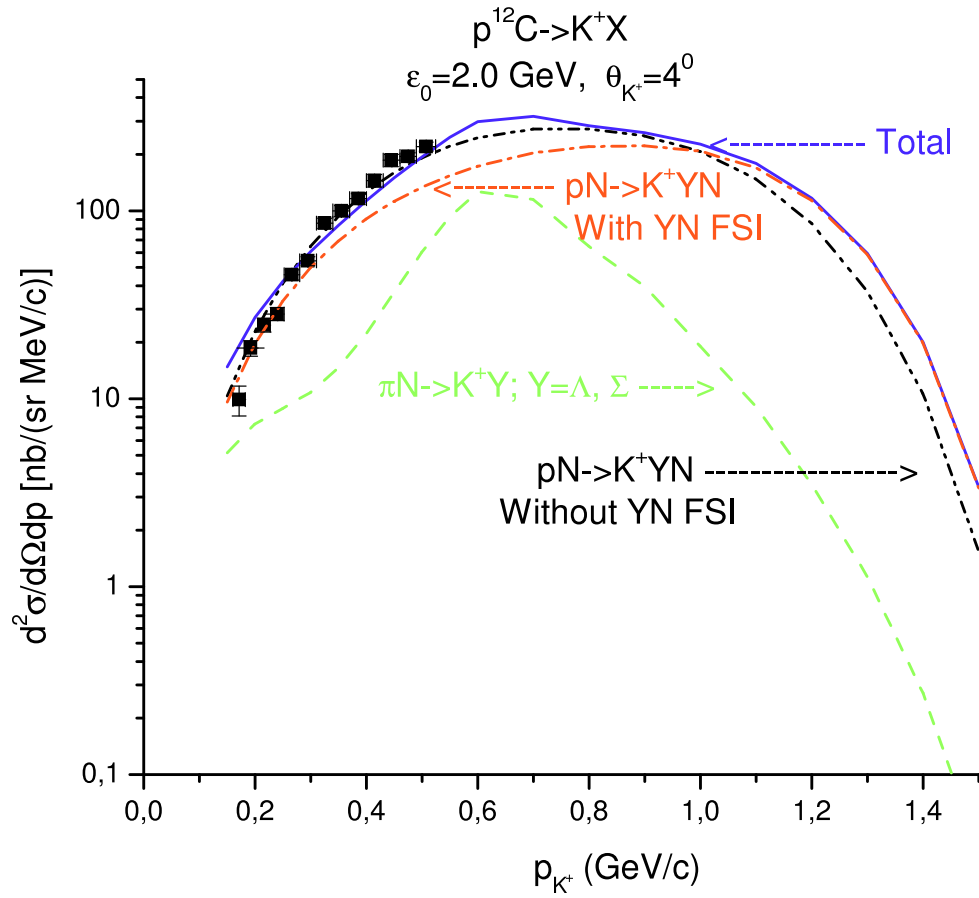


Figure 5: The same as in Fig. 4, but for 2.0 GeV beam energy.

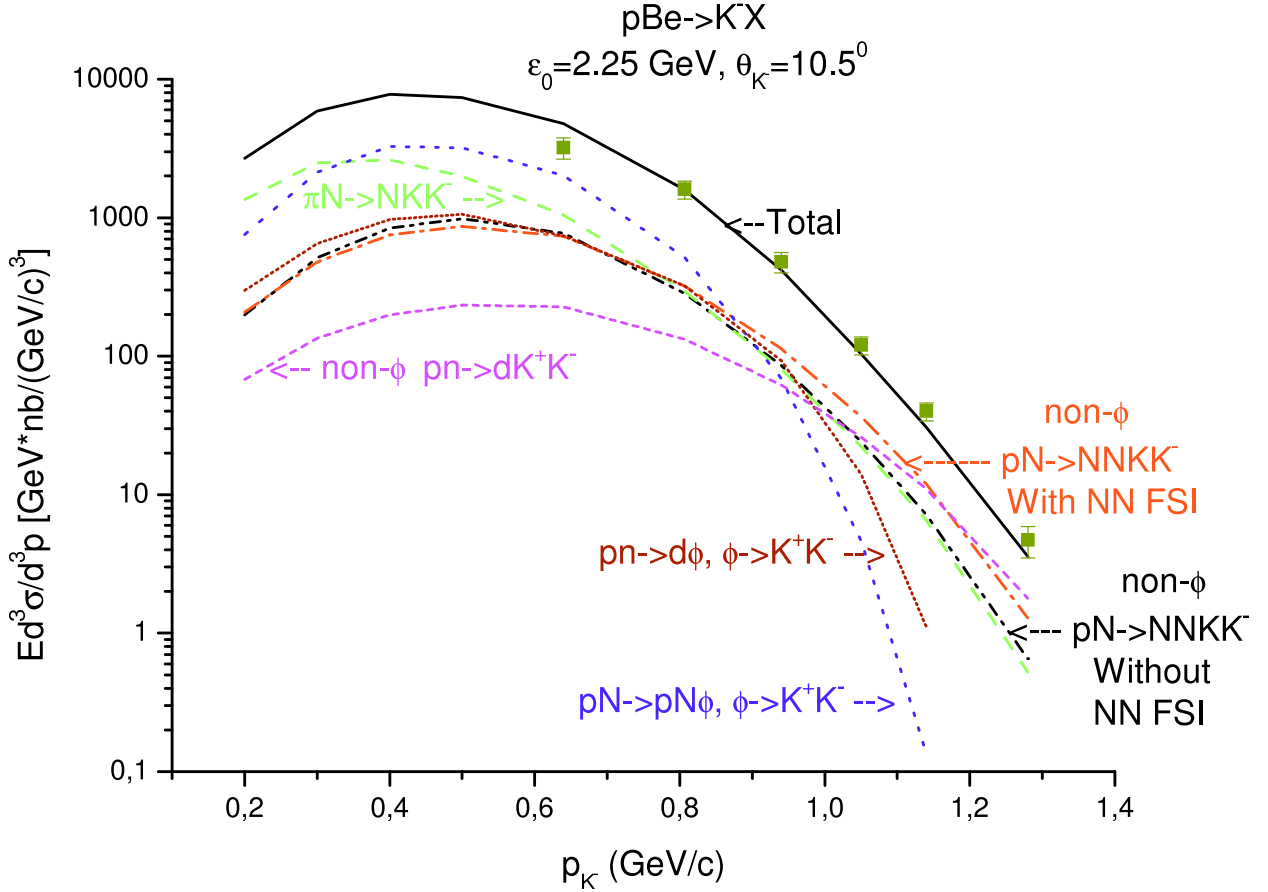


Figure 6: Invariant cross sections for the production of K^- mesons at an angle of 10.5° in the interaction of 2.25 GeV protons with the ${}^9\text{Be}$ nuclei as functions of antikaon momentum. The experimental data (full squares) are obtained at the ITEP accelerator (see Table 2). The curves show our calculation. The dashed lines with one and two dots show the calculation for the primary production process $pN \rightarrow NNKK^-$ with and without including the FSI effects among the outgoing nucleons. The dashed and short-dashed lines represent the calculation, respectively, for the secondary production process $\pi N \rightarrow NKK^-$ and direct non- ϕ $pn \rightarrow dK^+K^-$ channel. The dotted and short-dotted lines show the calculation for the secondary creation processes $pN \rightarrow pN\phi$, $\phi \rightarrow K^+K^-$ and $pn \rightarrow d\phi$, $\phi \rightarrow K^+K^-$. The solid line is the sum of the dash-dotted, dashed, short-dashed, dotted and short-dotted lines.

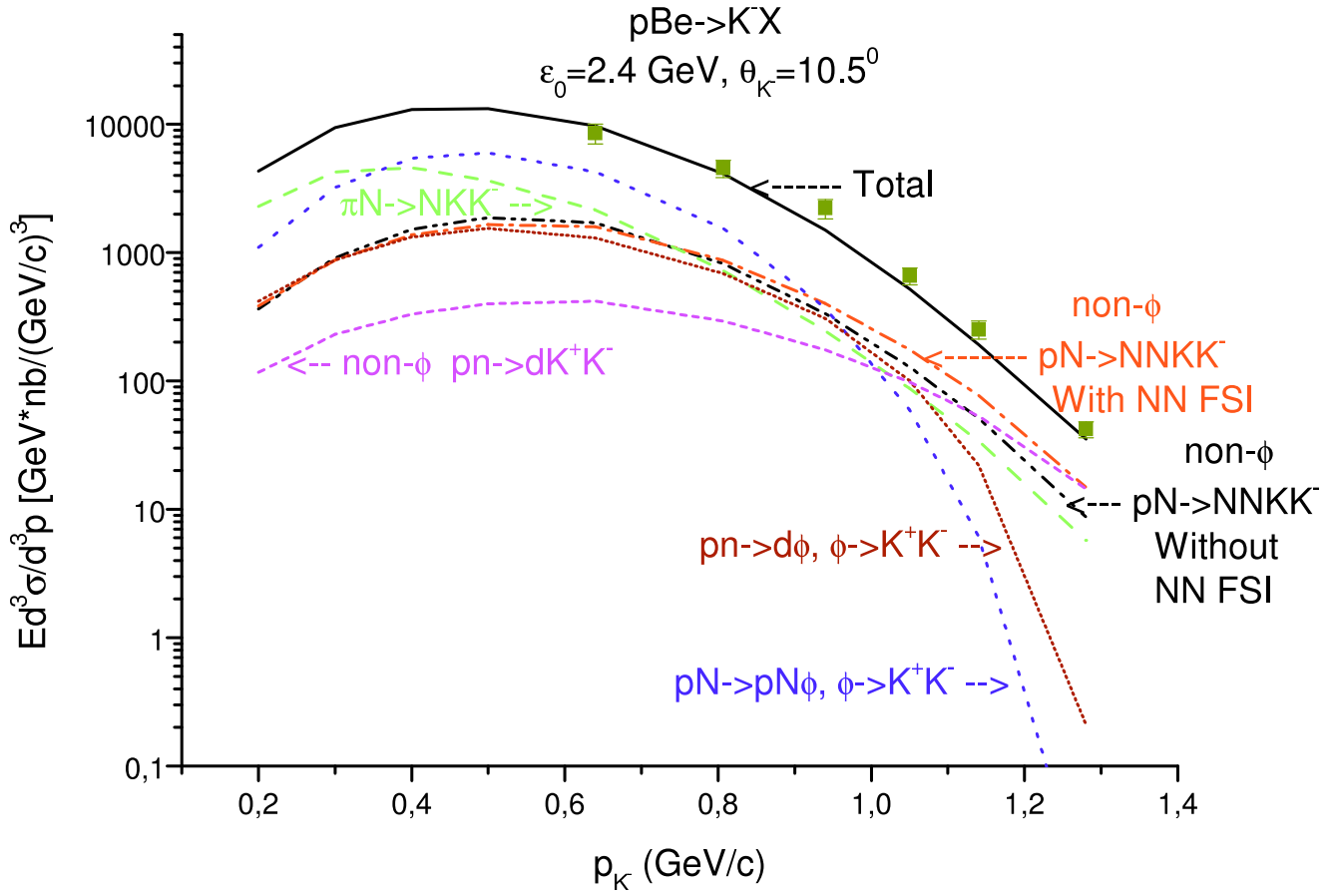


Figure 7: The same as in Fig. 6, but for 2.4 GeV beam energy.

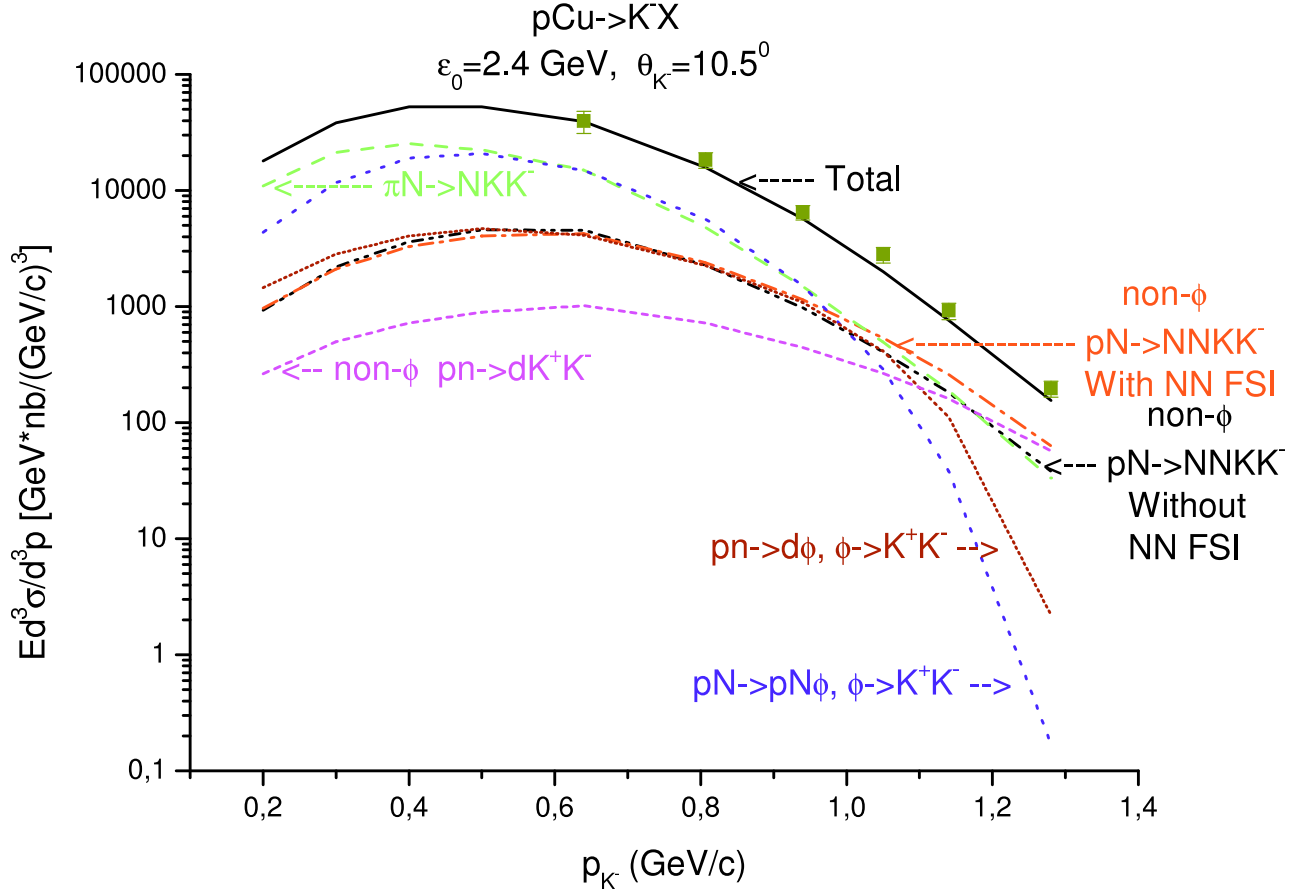


Figure 8: The same as in Fig. 6, but for the interaction of 2.4 GeV protons with the ^{63}Cu nuclei.

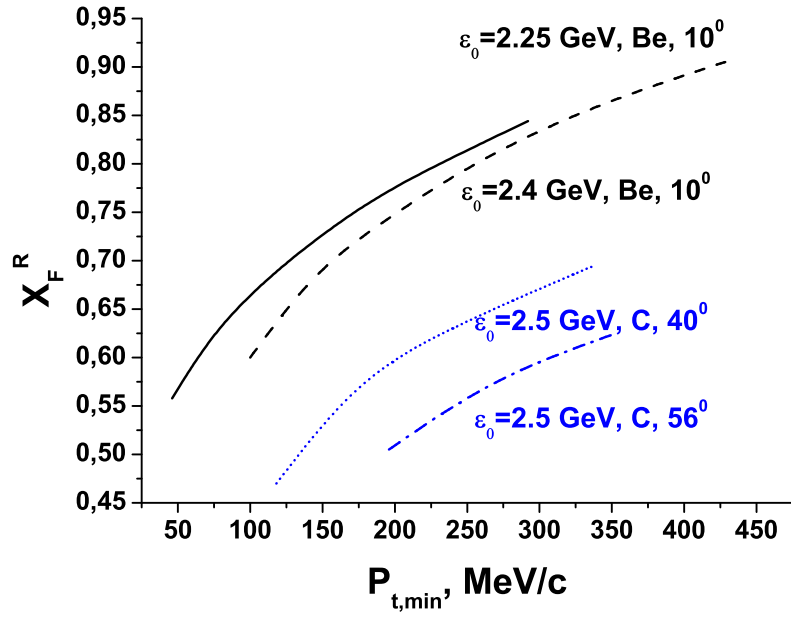


Figure 9: Radial Feynman variable X_F^R for the hyperon production as a function of $P_{t,min}$ calculated for the kinematical conditions of the present experiment (solid and dashed curves) and [18] (dotted and dash-dotted curves).